

Influence of electronic entropy on Hellmann-Feynman forces in *ab initio* molecular dynamics with large temperature changes

Ming Geng (耿明)^{1,2} and Chris E. Mohn^{1,2,3*}

¹Centre for Planetary Habitability (PHAB), University of Oslo, N-0315 Oslo, Norway

²Centre for Earth Evolution and Dynamics (CEED), University of Oslo, N-0315 Oslo, Norway and

³Department of Chemistry and Center for Materials Science and Nanotechnology, University of Oslo, Oslo 0371, Norway

(Dated: September 22, 2023)

The Z method is a popular atomistic simulation method for determining the melting temperature where a sequence of microcanonical molecular dynamics runs are carried out to target the lowest system energy where the solid always melts. Homogeneous melting at the limit of critical superheating, T_h , is accompanied by a drop in temperature as kinetic energy is converted to potential energy and the equilibrium melting temperature, T_m , can be calculated directly from the liquid state. Implementation of the Z method interfaced with modern *ab initio* electronic structure packages use Hellmann-Feynman forces to propagate the ions in the microcanonical ensemble where the Mermin free energy plus the ionic kinetic energy is conserved. The electronic temperature, T_{el} , is therefore *kept fixed* along the trajectory which may introduce some spurious ion-electron interactions in molecular dynamics runs with large changes in temperatures such as often seen in homogeneous melting and freezing processes in the microcanonical ensemble. We estimate possible systematic errors in the calculated melting temperature to choice of T_{el} for two main mantle components, the wide band-gap insulators SiO_2 and CaSiO_3 at high pressure. Comparison of the calculated melting temperature from runs where the $T_{el} = T_h$ and $T_{el} = T_m$ - representing reasonable upper and lower boundaries respectively to choice of T_{el} - shows that the difference in melting temperature is 200-300 K (3-5% of the melting temperature) for our two test-systems. Our results are in good agreement with previous large-size co-existence method and thermodynamic integration calculations, suggesting the CaSiO_3 and SiO_2 melts at around 6500 K (100 GPa) and 6000 K (160 GPa) respectively. The melting temperature decreases with increasing T_{el} due to the increasing entropic stabilisation of the liquid and the systems melts typically about 3 times faster in molecular dynamics runs with $T_{el} = T_h$ compared to runs where $T_{el} = T_m$. A careful choice of electron temperature in Born-Oppenheimer molecular dynamic simulations where the ions are propagated using Hellmann-Feynman forces with the Mermin free energy + the ionic kinetic energy being conserved, is therefore essential for the critical evaluation of the Z method and in particular at very high temperatures.

I. INTRODUCTION

Melting and solidification processes are ubiquitous in condensed matter physics and in the evolution of terrestrial bodies including our own Earth. Triggered by extended defects, grain boundaries or open surfaces, equilibrium melting occurs spontaneously at T_m when the free energy of the solid equals that of the liquid. Under certain conditions, however, a crystal can melt *homogeneously* at a much higher temperature, T_h , which represents the critical limit of superheating before melting is unavoidable [1, 2]. If a perfect periodic crystal in a molecular dynamics simulation is heated until $T \approx T_h$, spontaneous fluctuations (nucleation precursors) will form transient defects and liquid nuclei which trigger an irreversible rapid nucleation growth and melting. Although homogeneous melting is rare in nature, shock-induced homogeneous melting has been demonstrated in a number of experiments (see for example [3–7]).

The Z method explores the link between homogeneous and equilibrium melting using molecular dynamics simulations and has been widely used to estimate melting

temperatures for different materials [8–11] often at high temperatures and pressure where experiments are hazardous or impractical [12–17]. A number of molecular dynamics simulations are launched in the microcanonical (NVE) ensemble at different initial temperatures, T_{ini} , to target the lowest total energy, E_h , where the solid always melts. When the system melts at $E_h(T_h)$, the temperature decreases to the equilibrium melting temperature while the latent heat of melting gradually converts into potential energy. If we assume a linear variation of energy with temperature we can establish a relationship between T_h and T_m from the entropy of melting [1, 18]:

$$\frac{T_h}{T_m} - 1 = \frac{\Delta S_m}{C_V} \quad (1)$$

where C_V is the heat capacity at constant volume of the solid and ΔS_m is the entropy of melting. Eq. 1 can be approximated by $\ln 2/3$ assuming an ideal entropy of melting ($3k_B$ (per atom)) taken from a high-temperature limit of the Debye model and assuming that the heat capacity at constant volume is given by $k_B \ln 2$ (per atom) when $\Delta V_m/V \rightarrow 0$ [19].

Since the equilibrium melting temperature can be calculated at T_h from a homogeneous melting triggered typically by small defects, quite small simulation boxes (~ 100 atoms) are in general sufficient to accurately calcu-

* chris.mohn@kjemi.uio.no

late T_h and hence T_m from Eq. 1 [20]. The use of small simulation boxes therefore makes the Z method a potentially attractive "low-cost" method for the accurate calculation of melting temperatures [20–22]. By contrast, popular two-phase approaches to melting where the equilibrium melting process is mimicked by constructing a simulation box with a solid and a liquid phase in mechanical contact, often require large boxes to accommodate both solid and liquid phases and their interface [23, 24].

In addition, since T_m can be calculated from Eq. 1, there is no need for the explicit calculation of free energies which sometimes hamper the precision of thermodynamic integration [25, 26] and 2PT methods [27], especially when the solid and liquid free energy curves have very similar steepness near T_m [23, 28].

In spite of these advantages, recent studies have unveiled some artificial features that may hamper the Z method for the accurate calculation of melting temperatures, particularly under extreme conditions [21, 23]. Since the waiting time required for the solid to melt diverges in the limit where $T_{ini} \rightarrow T_h$, a waiting time analysis is often carried out at different $T_{ini} > T_h$ to estimate T_m from extrapolation to that of "infinite" waiting-time [21]. This analysis, however, may still require extensive statistics for the precise calculation of melting temperatures.

Moreover, Born-Oppenheimer *ab initio* molecular dynamics (BOMD) is typically performed in the NVE ensemble using Hellman-Feynman dynamics where the Fermi-Dirac electronic temperature is *kept fixed* in the MD simulation [29]. Although this implementation of the Z method ensures conserved dynamics [30, 31], large changes in temperature following melting and sometimes equilibration, may introduce systematic errors in T_m since the electronic temperature is kept fixed [23]. That is, if a BOMD NVE run with $E > E_h$ is launched with an T_{el} chosen near the melted liquid temperature ($T_{el} \approx T_m$), then T_{el} will be much lower than the temperature in the solid state (before melting). A too low electronic entropy may favour the stabilisation of the solid and prevent melting. This in turn will affect the estimated homogeneous melting temperature (T_h) and the "waiting time" for a solid to melt. The calculated equilibrium melting temperature may therefore be too high. On the other hand, if a BOMD run is launched with an electronic temperature chosen near the solid temperature before melting ($T_{el} \approx T_h$) a physically reasonable electronic-ionic interaction is ensured before melting. However, once the solid melts at constant volume, the temperature drops by $1 - T_m/T_h \approx \ln 2/3$ and the electronic entropy will be much *higher* than the liquid temperature, which usually favours an entropic stabilisation of the liquid. Hence, the melting temperature may be too low. Therefore, since the choice of electronic entropy affect ion dynamics in processes undergoing large temperature drops, such as melting in the microcanonical ensemble, addressing the sensitivity in T_m to the choice of T_{el} is crucial in order to benchmark the Z method for the accurate calculating of melting temper-

atures.

In this work, we thus investigate the role of electronic entropy on homogeneous melting for two main abundant mineral components in the Earth's interior CaSiO_3 and SiO_2 at high temperatures.

Ca-perovskite is the third most abundant mineral in the lower mantle and a main component of basaltic lithologies constituting more than 20% of recycled oceanic crust that is continuously being injected into the Earth's deep interior. A strong preferential partitioning of radioactive heat-producing elements into CaSiO_3 , such as U and Th, as well as key geochemical tracers, suggests that CaSiO_3 is the main storage minerals for many of these minority elements [32, 33]. Tracking the distribution of CaSiO_3 in the lowermost mantle is therefore essential to understand the evolution of the solid Earth which in turn requires the thermodynamic conditions of Ca-perovskite melting. Motivated by this, a number of computational studies have calculated melting curves for pure CaSiO_3 to lowermost mantle conditions [18, 23], but the agreement is not satisfactory. Here we attempt to contribute to tighten the constraints of CaSiO_3 melting at the lowermost mantle conditions.

Our second model system is SiO_2 . The solid-liquid phase boundary of SiO_2 at ultrahigh pressure is critical to our understanding of not only the Earth's evolution but also the formation of many super-Earths [34, 35]. High-pressure silica melting may also play an important role in core dynamics, as it has been suggested that silica may have crystallized from a Si-saturated proto-core during a chemical exchange with a basal magma ocean [36, 37]. In spite of a number of simulations and experimental results reported in the literature, the SiO_2 melting curve remains poorly constrained at very high pressure. Here we will attempt to contribute to resolving some of these outstanding discrepancies.

II. THEORY

The thermodynamic ensemble appropriate for the Z method is the microcanonical (NVE) ensemble with the volume, V , number of species N and the total system energy, E , kept fixed. The maximum energy along the solid branch of the isochore, E_h , is the same as the lowest energy along the liquid branch:

$$E_{\text{sol}}(V, T_h) = E_{\text{liq}}(V, T_m). \quad (2)$$

To locate $E_{\text{sol}}(V, T_h)$ and hence $E_{\text{liq}}(V, T_m)$, a sequence of NVE MD runs are carried out with different initial temperatures. Since the waiting time for the solid to melt diverges when $T \rightarrow T_h$, the calculated melting temperature will always represents an upper bound to the "true" melting temperature. To avoid extremely long MD runs in the vicinity of T_h , the melting temperature is calculated from an extrapolation of the distributions of waiting times using

$$\langle \tau \rangle^{-1/2} = A(T_{\text{liq}} - T_m) \quad (3)$$

where "A" is a parameter, τ is the waiting time for a solid to melt at a given total energy and T_{liq} is the liquid temperature of the system after melting. Since $T_{\text{liq}} = T_m$, when $E = E_h$, the melting temperature can be found at infinite waiting time i.e. at the point of intersection where $\langle\tau\rangle^{-1/2} = 0$.

We use *ab initio* Born-Oppenheimer MD to propagate the ions where the electronic energy is minimized at each step along the trajectory. Note that the usual Hellmann-Feynman forces do not conserve the total system energy, $E = U + K$ where U is the internal DFT energy and K is the kinetic energy of the ions. This is because the energy functional is non-variational with respect to changes in partial orbital occupancies along the MD trajectory.

To avoid additional contributions to the Hellmann-Feynman forces due to the variation in the band occupancies along the ionic trajectory the quantity " $K + \Omega$ ", rather than the total energy, is conserved in the MD run where Ω is the Mermin free-energy [30, 31, 38]

$$\Omega = U - T_{\text{el}}S_{\text{el}} \quad (4)$$

with

$$S_{\text{el}} = -k_B \sum_i [f_i \ln f_i + (1 - f_i) \ln(1 - f_i)]. \quad (5)$$

S_{el} is the electronic entropy and f_i is the electron occupancy of band i calculated using Fermi-Dirac statistics:

$$f_i = F\left(\frac{\epsilon_i - E_{\text{fermi}}}{\sigma}\right), \sum_0^{N_i} f_i = N \quad (6)$$

where F is the usual (Fermi-Dirac) smearing function, ϵ_i is the eigenvalue of band i , E_{fermi} is the Fermi level and $\sigma = k_B/T$ is the smearing broadening.

Ionic dynamics may be sensitive to the choice of electronic temperature when the ions are propagated using Hellmann-Feynman forces, in particular when the temperature changes are large such as during equilibration and melting in the *NVE* ensemble. Electronic temperature may therefore affect the melting processes for semiconductors and insulators even though the fractional occupancies of the conduction bands, remain small during these temperature changes.

We can estimate the sensitivity in the calculated T_m to choices of T_{el} by comparison of the melting temperature calculated using $T_{\text{el}} \approx T_h$ with that calculated $T_{\text{el}} \approx T_m$. These choices of T_{el} provide reasonable upper and lower bounds to the calculated melting temperature in the microcanonical ensemble when the Hellmann-Feynman forces are used for the ionic propagation with $K + \Omega$ being conserved.

If changes in T_{el} can not be ignored, the usual conservation law including the Mermin functional in the form of Eq. 4 must be replaced, but the forces will then include contributions arising due to changes in the partial orbital occupancies along the microcanonical Born-Oppenheimer trajectory. It is important to note, however, that the time evolution of orbital occupancies due

to large temperature changes may be only correctly described by the time-dependent Schrödinger equation.

A possible strategy to calculate T_m using the Z method is to adjust T_{el} along the ionic trajectory to match the average (ionic) temperature in the previous N time-steps [23]. Although this "update scheme" does not ensure conserved dynamics, the average ensemble temperature before and after adjustment is in general expected to be small. In this approach, the time-dependent Schrödinger equation is thus approximated by a sequence of BOMD *NVE* simulations.

III. COMPUTATIONAL DETAILS

All BOMD simulations are performed with the Vienna *ab initio* simulation package (VASP) [39, 40], using the projector augmented wave (PAW) method [41, 42]. We use the generalized gradient approximation (GGA) where the exchange-correlation contribution to the energy is parameterized using the PBE [43] functional for SiO_2 and the AMO5 functional [44] for CaSiO_3 . The electronic configurations were: $[\text{He}]2s^2 2p^4$ for O, $[\text{Ne}]3s^2 3p^2$ for Si and $[\text{He}]3s^3 p^6 4s^2$ for Ca. The energy cutoff for the plane wave was 700 eV for SiO_2 and somewhat lower, 500 eV, for CaSiO_3 to compare directly with previous CaSiO_3 DFT studies [18, 23].

In all runs, the atoms were placed at their ideal crystallographic sites i.e. the $1b$, $1a$ and $3d$ positions for Ca, Si and O atoms respectively of the $Pm3m$ space group (CaSiO_3). SiO_2 MD runs were started from the ideal cubic pyrite-type structure ($Pa\bar{3}$) optimized to target an equilibrium pressure ~ 160 GPa. This is probably slightly below the stability field of the pyrite structured SiO_2 near the melting curve [34], but in order to compare directly with results in Ref. [22, 35] we use pyrite rather than seifertite. The estimated melting point when pyrite is used as the crystal structure is only slightly lower compared to that found using seifertite. [22, 35]. For CaSiO_3 we use a cubic 135 atoms simulation box which is the same as that used in previous computational studies of CaSiO_3 melting [18, 23] allowing for a direct comparison with these studies. For SiO_2 the simulation box contained 96 atoms.

Melting simulations are carried out in the *NVE* ensemble with a timestep of 0.5 fs for SiO_2 and 1 ps for CaSiO_3 . The smaller timestep for SiO_2 was chosen to minimize the energy fluctuation. All runs used in the calculation of the waiting time were carried out until melting plus an additional 5-20 ps to calculate the average liquid temperature.

The waiting time analysis were performed based on between 8 and 20 different simulations at a given (E, V) where, in each run, the forces were taken from a Maxwell-Boltzmann distribution. Close to the equilibrium melting temperature we performed typically around 20 MD runs at a given (E, V) to ensure that sufficient statistics were collected in order to calculate $\langle\tau\rangle$ using Eq. 3. Plots

of the convergence of the estimated melting temperature with number of configurations are shown in supplementary information. This analysis shows that about 8-10 MD runs, for a given initial temperature, is sufficient to converge the melting temperature to less than 100 K. All MD calculations launched below E_h , lasted for at least 10 ps and close to T_h the MD simulations typically ran for more than 100 ps.

For SiO_2 , the T_{el} are 6000 K, 7000 K and 8000 K where 6000 K is expected, after test-calculations, to lie close to T_m whereas 8000 K will lie close to T_h . Similarly, for CaSiO_3 the waiting time analysis was carried out at $T_{el} = 6500$ K and 9000 K which are expected to be close to T_m and T_h respectively. To simulate melting with negligible contribution from the electronic entropy we used a Gaussian scheme [29] with a very low value of the smearing parameter (i.e. $\sigma_{\text{Gaussian}} = 0.03$ eV). The Gaussian smearing method is better designed to avoid instabilities arising from fluctuations in orbital occupancies at low values of σ (low temperatures) which often hamper the Fermi-Dirac method during energy minimizations. The Gaussian smearing has the functional form $\frac{1}{2}(1 - \text{erf} \frac{\epsilon - \mu}{\sigma})$ and the link between the two schemes is given by the ratios of the full width at half maximum, FWHM, as:

$$\frac{\text{FWHM}_{\text{FermiDirac}}}{\text{FWHM}_{\text{Gaussian}}} = \frac{\cosh^{-1}(\sqrt{2})}{\sqrt{\ln 2}}. \quad (7)$$

IV. RESULTS AND DISCUSSION

A. Influence of electronic entropy on ionic dynamics

In Fig. 1 we illustrate the sensitivity to changes in electronic temperature on the melting dynamics for silica where the initial ionic temperatures are *the same* in all runs. In the extreme case where the electronic temperature is the same as the initial temperature in the MD runs ($T_{el} = T_{ini} = 18000$ K), SiO_2 always melts rapidly and instantaneously in less than 0.5 ps. On the contrary, in runs with negligible contribution from electronic entropy (i.e. with $\sigma_{\text{Gaussian}} = 0.03$ eV), melting is rare and we observed only one incidence of melt-nucleation in all our 20 runs which lasted 10 ps each.

In simulations with "intermediate" T_{el} , close to either the homogeneous or the equilibrium melting temperatures (i.e. with $T_{el} = 8000$ K or $T_{el} = 6000$ K respectively), the system with $T_{el} = 6000$ K melted markedly slower compared to those with $T_{el} = 8000$ K and the waiting time was much longer. We found that the average waiting time was 2.7 ps when $T_{el} = 8000$ K $\approx T_h$ and markedly longer by a factor of about 3 when $T_{el} = 6000 \approx T_m$. See also the discussion about distributions of the waiting time in the supplementary information. Interestingly, when $T_{el} = 6000$ K, we observe that the temperature sometimes drops markedly indicating possibly the formation of melt nuclei, but the system

quickly reverted to its original (solid) state. This is seen as a small "bump" in the temperature/pressure evolution in Fig. 1 at about 2.0-2.5 ps. Solid-liquid "oscillations" are often seen in runs where the energy is close to the target homogeneous melting energy using small simulation boxes with large temperature fluctuations [21] and will be discussed more in the supplementary information.

The influence of electronic entropy on properties is also seen in Fig. 2 where two isochores with different electronic temperatures are drawn. Here, the initial ionic temperature in the MD runs is systematically increased from 8000 K to 30000 K. The isochores with an high electronic temperature i.e. close to T_h (i.e. with $T_{el} = 8000$ K) deviates strongly from the one with negligible contributions from electronic entropy (i.e. $\sigma_{\text{Gaussian}} = 0.03$ eV).

B. Choice of electronic temperature in *ab initio* MD runs

The sensitivity in melting temperature to choice of T_{el} illustrated above for SiO_2 and discussed in the supplementary information suggests that BOMD runs in the *NVE* ensemble where the ions are propagated using the Hellmann-Feynman forces with $\Omega + K$ being conserved may introduce some errors due to changes in electronic interactions following large drops in temperature $\approx \ln 2/3 \times T_h$. This is seen in the Z plots and the waiting-time analysis in Fig. 3 and 4 as well as in Table I for both SiO_2 and CaSiO_3 . When T_{el} is kept fixed at some value near T_m , the calculated equilibrium melting temperature will be markedly higher compared to that if T_{el} is close to the homogeneous melting temperature. The calculated melting temperatures with $T_{el} \approx T_m$ at around 100 GPa (CaSiO_3) and 150 GPa (SiO_2) are about 300 K and 200 K higher respectively than those calculated with $T_{el} \approx T_h$. This corresponds roughly to 10% of the temperature drop accompanying melting. We expect that these absolute errors increase with increasing melting temperature and pressure since the temperature drop accompanying melting increases with increasing T_h .

A key question is therefore: what is the best choice of electronic temperature in the MD runs to minimize the errors in the calculated T_m when the ions are propagated using Hellmann-Feynmann forces with $\Omega + K$ being conserved? If we choose an electronic temperature very close to T_h in MD runs with $E = E_h$, the electronic temperature is very close to the (ensemble) average temperature before the system eventually melts. Runs with $T_{el} \approx T_h$ therefore enables the accurate calculation of T_h as well as the waiting time and implies that MD runs where $T_{el} < T_h$ (if, say $T_{el} = T_m$) give too high homogeneous melting temperatures.

Although $T_{el} \approx T_h$ (with $E \approx E_h$) enables the accurate calculation of T_h , the melting temperature may be severely underestimated. This is because T_{el} is much larger than the liquid (ionic) temperature which, in gen-

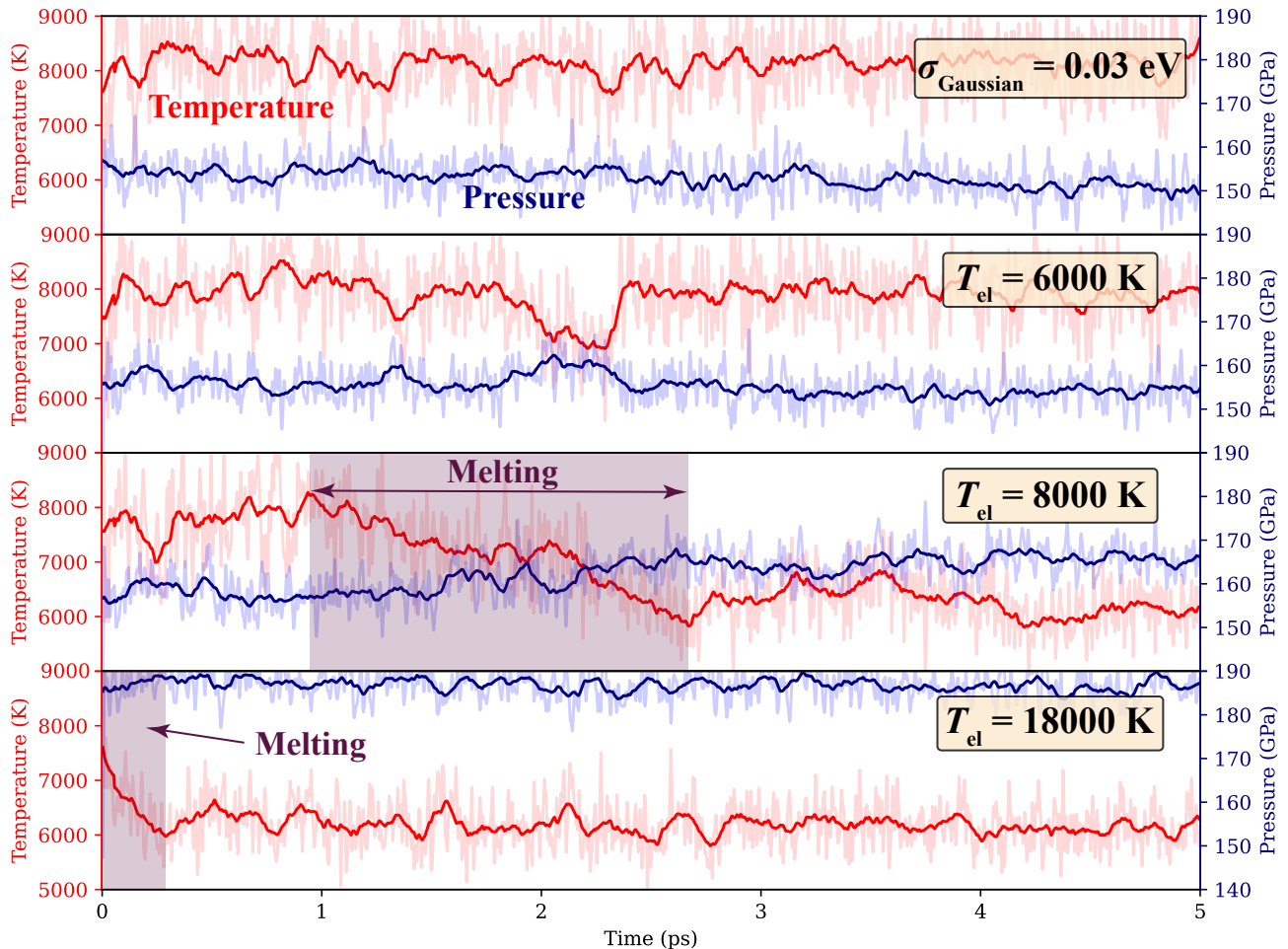


FIG. 1. Temperature (red) and pressure (blue) evolutions along snapshots of *ab initio* MD trajectories for SiO₂ with different T_{el} . The thin lines show dumps every time-step whereas the thick lines are averaged properties over the previous 100 time-steps. All MD runs are carried out with the same initial temperature ($T_{ini} = 18000$ K) where the atoms are distributed at their equilibrium lattice positions before we launch the MD run. A Gaussian smearing broadening scheme with $\sigma_{\text{Gaussian}} = 0.03$ eV is used to represent simulations with a negligible contribution to electronic entropy on the ionic dynamics. The shaded area shows the melting process.

eral, favours an entropic stabilization of the liquid over the solid and hence the calculated melting temperature will be too low. If we rather chose $T_{el} \approx T_m$ - which is the lowest temperature on the isochore and therefore represents a reasonable lower bound to choice of T_{el} - the homogeneous melting temperature and possibly the equilibrium melting temperature will be *overestimated*. Calculations where T_{el} is chosen to target either T_m or T_h , therefore, provide reasonable *upper and lower bounds* respectively to the true melting temperature.

C. CaSiO₃ melting

As shown in Table I, our melting temperatures are in very good agreement with a previous Z method study [23]

and also in excellent agreement with those from thermodynamic integration and two-phase calculations [23]. The inclusion of electronic entropy is essential for the accurate calculation of melting temperature for CaSiO₃, in agreement with that found for other wide band gap insulators such as MgO [45]. That is, the calculated T_h and T_m without contribution from the electronic entropy are about 1000 K and 650 K higher respectively than those calculated using $T_{el} = 6500$ K. We find that that the melting temperature is around 6300 K (with $T_{el} = 9000$ K) and 6600 K (with $T_{el} = 6500$ K). As discussed above, the discrepancy between the calculated melting temperature using $T_{el} = 6500$ K with that calculated using $T_{el} = 9000$ K is non-negligible for the accurate calculation of melting temperature. This places some constraints on the accuracy of the Z method interfaced with BOMD where $\Omega +$

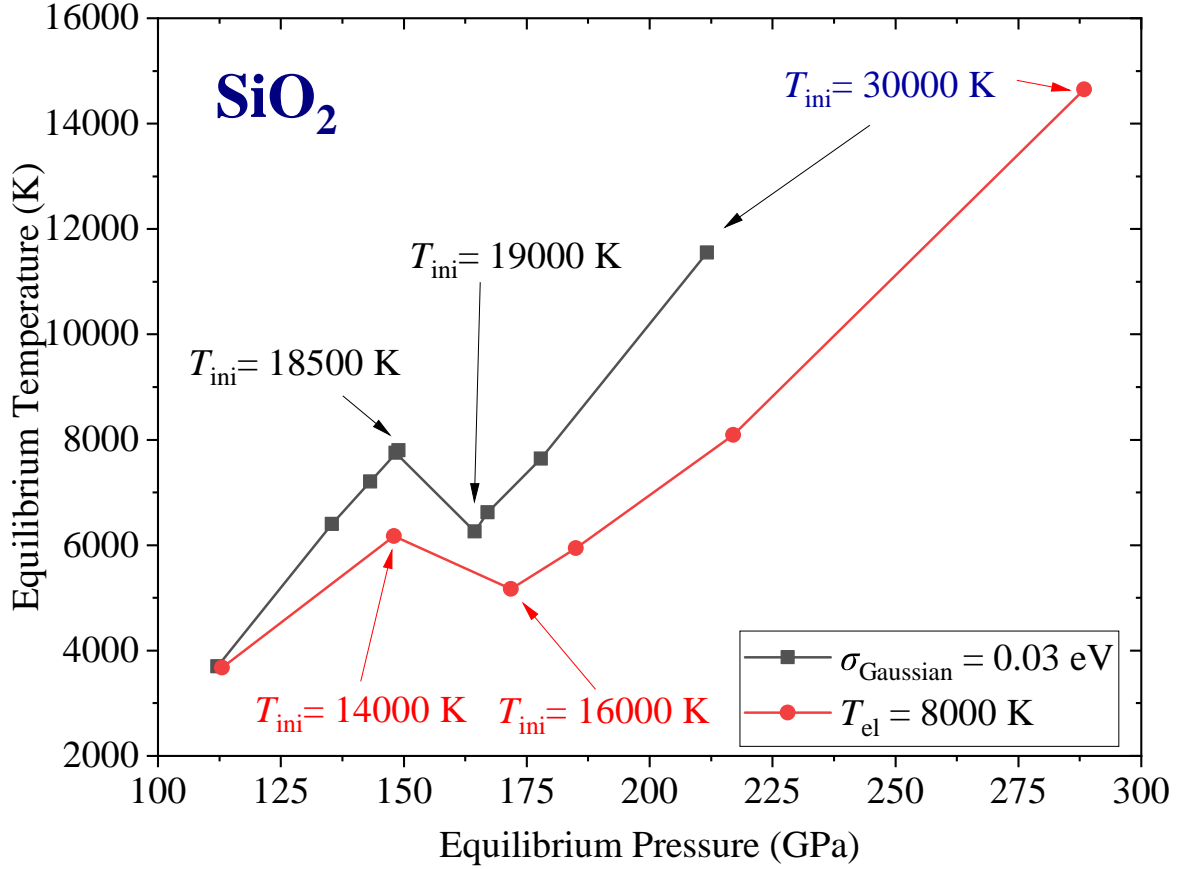


FIG. 2. Two isochores with different electronic temperatures. The black curve is runs where $\sigma_{\text{Gaussian}} = 0.03$ eV and the red curve is runs where $T_{\text{el}} = 8000 \approx T_{\text{m}}$. The initial temperatures are in the range 8000 K to 30000 K with the ions initially placed at their ideal lattice positions before we launched the MD simulations which ran for 20 ps each.

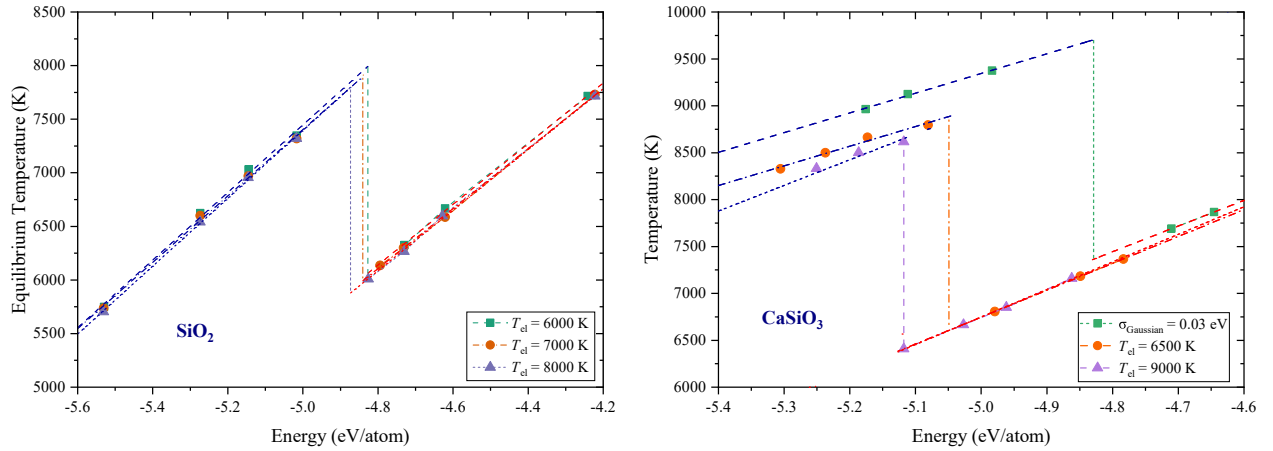


FIG. 3. Solid (blue) and liquid (red) branches in MD-NVE runs for SiO_2 (left) and CaSiO_3 (right). For SiO_2 , $T_{\text{el}} = 6000$ K, 7000 K and 8000 K whereas for CaSiO_3 , T_{el} are 6500 K and 9000 K. In addition, we plot the result for CaSiO_3 with a Gaussian smearing scheme using $\sigma_{\text{Gaussian}} = 0.03$ eV. The homogeneous melting temperatures are calculated from an intersection of a linear extrapolation of the solid branch runs and a vertical line drawn from the equilibrium melting point (calculated using Eq. 3). The resulting homogeneous melting temperatures may therefore represent an upper bound to the "true" homogeneous melting temperature since the slope of the solid branch typically decreases near T_{h} [20, 23]. Values of T_{h} are reported in Table I.

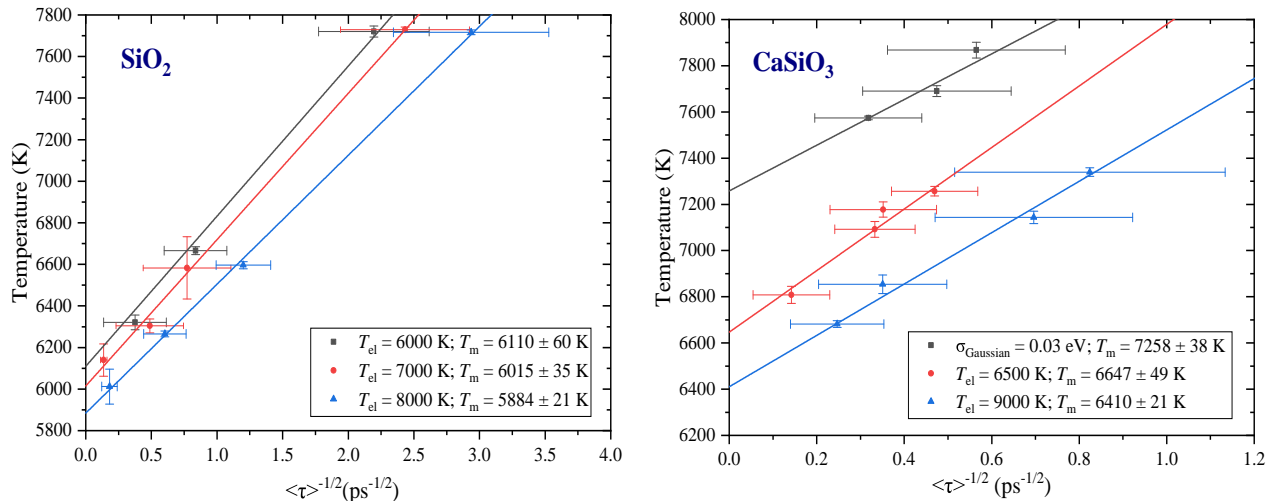


FIG. 4. The calculated melting temperature using Eq. 3 for different choices of electronic temperatures. For SiO_2 , $T_{\text{el}} = 6000$ K, 7000 K and 8000 K whereas for CaSiO_3 , T_{el} are 6500 K and 9000 K. In addition, we plot the waiting time for CaSiO_3 using a Gaussian smearing scheme with $\sigma_{\text{Gaussian}} = 0.03$ eV. The resulting estimated equilibrium melting temperatures are reported in Table I along with the standard error. The horizontal and vertical error bars reported are the mean errors of the waiting time and temperatures respectively.

K is conserved and the forces are propagated using the Hellmann-Feynman forces in the NVE ensemble.

Choice of electronic entropy could therefore possibly explain the large discrepancy of more than 1000 K between our melting point and that of a recent Z method study [18] which was carried out at the same thermodynamic conditions as here. We use the same exchange-correlation functional to DFT as that employed in Ref. [18], but are unable to reproduce their melting point unless we set $T_{\text{el}} = T_{\text{ini}}$. Ref. [18], however, do not report values of T_{el} so no firm conclusions can be drawn.

D. SiO_2 melting

There are not many experimental studies of SiO_2 that report melting temperatures to very high pressure. Results from a recent high-pressure experimental study [48] was fitted to an equilibrium melting curve to about 500 GPa ($T_{\text{m}}(P) = 1968.5 + 307.8 \times P^{0.485}$) suggesting that SiO_2 melts at around 5540 K at 157 GPa. This is slightly lower than that calculated from a Z method simulation [35], where the melting temperature was estimated to be 5850 K at 132 GPa. By contrast, a recent Diamond Anvil Cell (DAC) experiment [49, 50], suggests a markedly higher melting curve compared to those mentioned above and the Clapeyron slope is also much steeper in the pressure region 120-150 GPa compared to that reported by e.g. Millot *et al* [48]. The melting curves from two molecular dynamics simulations [46, 47] using two-phase co-existing methods are in overall good agreement with that from the DAC study [49, 50], but without the rapid change in the Clapeyron slope seen in the DAC experi-

ment at around 120 GPa.

Our calculated melting temperatures reported in Table I are in overall good agreement with previous computational predictions at similar pressures [46, 47]. The calculated melting temperature reported using $T_{\text{el}} = 8000$ K, for example, is 5776 K. This is only slightly lower compared to those of Refs. [46] and [47] which are 5990 K and 5986 K respectively. Of note is that the good agreement with that reported by Usui and Tschuchia [47] may be fortuitous because a very small two-phase simulation box containing only 48 atoms for each phase was used in Ref. [47]. Such a small box has a boundary that is of similar size as the solid and liquid portions, and many runs are needed at a given (E,V) to precisely determine the melting points [51]. Our result also suggests that the predicted equilibrium melting curve reported from a shock experiment study [48] may be too low since it is assumed that stishovite is able to crystallize at the time-scale of the experiment and the melting curve is therefore drawn at the bottom of the liquid branch of the Hugoniot. If, however, stishovite is unable to crystallize at the time-scale of the shock experiment (i.e. within a few nanoseconds), the melting temperature reported in Ref. [48] may be underestimated as suggested by [52]. This interpretation is consistent with our calculated melting point.

As discussed above, the calculated melting temperature using $T_{\text{el}} = 8000$ K is slightly less than 200 K lower than that calculated using $T_{\text{el}} \approx T_{\text{h}} \approx 6000$ K. This difference in the calculated melting temperature is of similar size compared to that found for CaSiO_3 at similar conditions and confirms that the Z method may be hampered by some artificial feature for the accurate calculations of melting temperature with the Mermin free energy

System	Method	T_{el} (K)	P (GPa)	T_h (K)	T_m (K)	Ref.
CaSiO ₃	Z-Method	9000	103.7±2.6	8873±42	6410±21	This work
	Z-Method	6500	103.0±2.5	8652±25	6647±49	This work
	Z-Method	~0	105.2±3.0	9605±11	7258±38	This work
	Z-Method	adjust ^a	102.6±2.7	8506	6517	This work
	Z-Method	adjust ^b	105±3.3	8806	6493	Hernandez <i>et al.</i> 2022 [23]
	Z-Method	not reported	103.0±0.2	7120	5200	Braithwaite <i>et al.</i> 2019 [18]
	large-size co-existence		≈103		6582	Hernandez <i>et al.</i> 2022 [23]
	Thermodynamic Integration 2-Phase thermodynamics		≈103		6433	Hernandez <i>et al.</i> 2022 [23]
SiO ₂	Z-Method	6000	164±4.3	8058±39	6110±60	This work
	Z-Method	7000	164±4.3	7899±30	6015±35	This work
	Z-Method	8000	166±4.3	7789±17	5884±21	This work
	Z-Method	adjust ^a	169±4.3		6044	This work
	Coexist		153.8		5990	Benlonoshko <i>et al.</i> 1995 [46]
	Coexist		157.6		5986	Usui <i>et al.</i> 2010 [47]
	Shock Experiment		157.0		5543	Millot <i>et al.</i> 2015 [48]
	Z-Method	not reported	132.3		5852	González-Cataldo <i>et al.</i> 2016 [35]
	DAC Experiment		117		≈6200	Andrault <i>et al.</i> 2022 [49]

TABLE I. Calculated melting temperature for CaSiO₃ and SiO₂ using the Z method together with previous values reported in the literature at similar pressure (i.e. about 103 GPa for CaSiO₃ and 160 GPa for SiO₂). In the simulation where $T_{el} \sim 0$ we used Gaussian smearing, $\sigma_{\text{gauss}} = 0.03$ eV, for the partial occupancies of the one-electron orbitals. In the simulation from Ref. [23] where T_{el} is labelled as "adjust^b", the Fermi-Dirac smearing was updated about every 1 ps along the MD trajectory to match the average temperature in the previous ~ 1 ps, as discussed in Ref. [23]. In "adjust^a" we update the electronic entropy only once along the MD trajectory after about 25 ps of propagation in the liquid state.

+ ionic kinetic energy being conserved along the Born-Oppenheimer MD-NVE trajectory with T_{el} kept fixed.

E. Sensitivity to changes in electronic entropy on the waiting time analysis

The waiting time for the solid to melt is correctly described if we chose $T_{el} \approx \langle T \rangle_{\text{sol}}$ after equilibration (i.e. if, for example, $T_{el} = T_h$ when $E = E_h$). However, since the melting temperature is in general underestimated with $T_{el} = T_h$, interpolation to infinite waiting time using Eq. 3 gives a too low equilibrium melting temperature when $\langle \tau \rangle$ is extrapolated to infinite waiting time. However, if we use a lower T_{el} (i.e. if we chose $T_{el} = \langle T \rangle_{\text{liq}}$) the waiting time for the system to melt will be too slow. This implies that $\langle \tau \rangle^{-1/2}$ should be shifted to lower temperatures indicating that the melting temperature calculated from the intersection $\langle \tau \rangle^{-1/2} = 0$ will be overestimated. The estimated melting temperatures from a waiting time analysis with $T_{el} \approx T_m$ and $T_{el} \approx T_h$, therefore, provide reasonable upper and lower bounds respectively to the "true" equilibrium melting temperature. These differences (~ 200 - 300 K) are much larger than the standard errors from the waiting time analysis (reported in Table I) which, in our case, are always less than 60 K. Convergence plots of the calculated melting temperatures using Eq. 3 with number of MD runs show that only a few tens of MD calculation are needed for the accurate

calculation of melting temperatures (see supplementary information).

To further understand the role of electronic entropy on the Hellmann-Feynman dynamics we can follow a similar strategy as in Ref. [23] by adjusting the electronic entropy along the MD trajectory to match the new average ionic temperature after transition to the liquid state. We thus pick one of the MD runs with $T_{el} \approx T_h$ and a total energy which is marginally higher than E_h . Using CaSiO₃ as an example, we expect that the average liquid temperature is close to the equilibrium melting temperature estimated from Eq. 3. Indeed, $\langle T \rangle$ after melting is 6408 K at ~ 105 GPa, which is within the error-bars of T_m (6410 K \pm 21 K). The simulation was then restarted after 25 ps of propagation in the liquid state with a new electronic temperature chosen to match the average liquid temperature. In Fig. 5 (top panel) we show the temperature evolution of this restarted run (blue). The total energy increased by about 1% accompanied by a temperature increase of about 100 K to 6517 K (labelled as "adjust" in Table 1). The $\langle T \rangle_{\text{liq}}$ from this relaunched MD run (blue line) is higher and lower respectively than the melting temperature reported in Table I for $T_{el} = 9500$ K and $T_{el} = 6500$ K respectively. This confirms that $T_{el} \approx T_h$ and $T_{el} \approx T_m$ represent reasonable upper and lower bounds to the "true" melting temperature

Fig. 5 for SiO₂ also demonstrates that changes in electronic entropy can have a substantial impact on the ionic dynamics. Here we relaunched a simulation by changing the

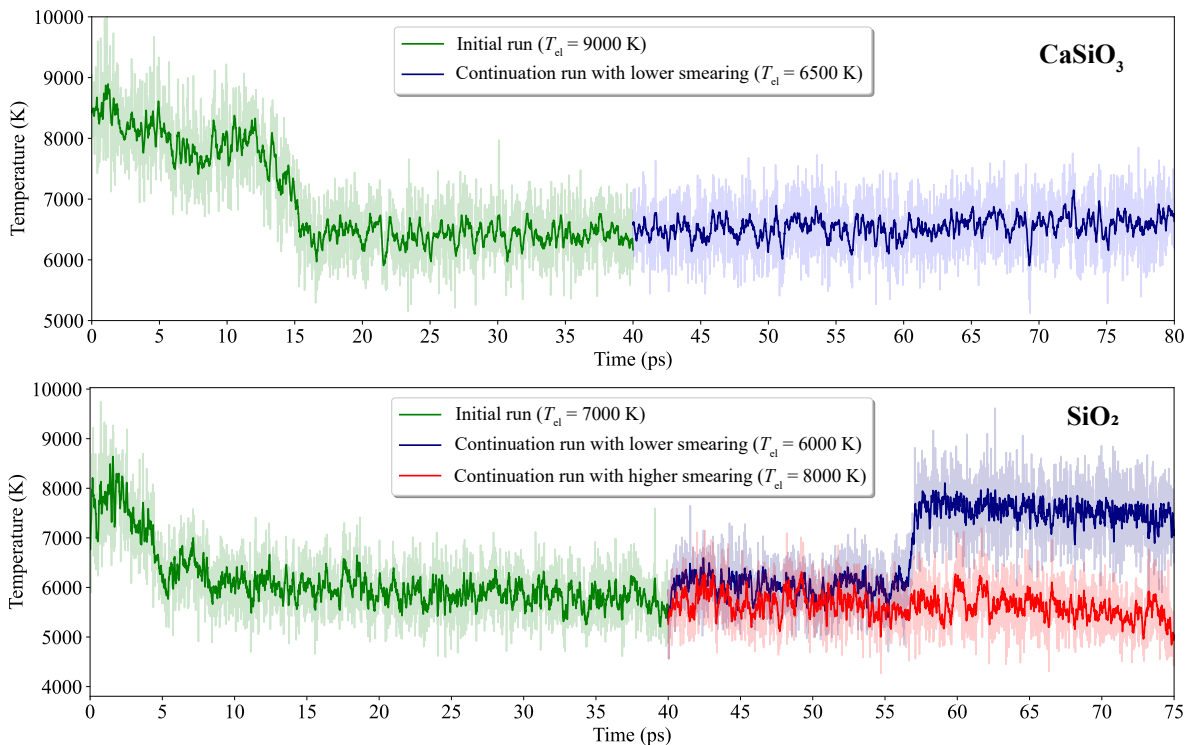


FIG. 5. Blue and red lines are continuation runs after about 40 ps of simulations (green lines). These continuation runs restarted with the same atomic positions and forces as the last step of the initial (green) run, but with different electronic temperatures. For CaSiO_3 , the MD run was initially launched with $T_{el} = 9000$ K (green line) and then restarted with $T_{el} = 6500$ K (blue line). For SiO_2 , we started with $T_{el} = 7000$ K (green line) and then continued with $T_{el} = 6000$ K (blue line) and 8000 K (red line).

electronic temperatures from 7000 K (green line) to $T_{el} = 6000$ K (blue line) or $T_{el} = 8000$ K (red line). Whereas the MD run with $T_{el} = 6000$ K *recrystallized* after about 15 ps of propagation in the liquid state the simulation with $T_{el} = 8000$ K remained stable in the liquid phase until the run was terminated after more than 35 ps.

V. CONCLUSIONS

In this work, we used the Z method together with *ab initio* Born-Oppenheimer molecular dynamics to calculate the melting temperature for SiO_2 and CaSiO_3 at outer core and lower mantle conditions respectively with simulation boxes containing ~ 100 atoms only. The calculated melting temperature for CaSiO_3 is in excellent agreement with results from previously reported two-phase co-existence calculations and thermodynamic integration and is substantially higher than that calculated in a previous *ab initio* study using the Z method [18]. A possible explanation for this discrepancy has been discussed. The calculated melting temperature for SiO_2 is also in overall good agreement with previous computational work carried out at similar pressure and temperature suggesting that the estimated equilibrium melting

curve reported in Ref. [48] may be too flat.

One of the great advantages with the Z method compared to other popular methods to melting, such as two-phase simulations and thermodynamic integration, is that the equilibrium melting temperature can be accurately calculated using small or modest-sized simulation boxes. This is because melting near T_h is in general triggered by the formation of defects and small liquid clusters which can be embedded in a small simulation box [20]. Moreover, since the melting temperature is obtained from the relationship between T_h and T_m using Eq.1, the Z method avoids the calculation of free energies which can be extremely tedious and expensive. The Z method can easily be implemented and interfaced with popular *ab initio* simulation software such as VASP [39, 40] and is embarrassingly parallelizable.

In spite of many appealing advantages compared to other methods to melting, the Z method appears to be hampered by some artificial features which needs to be much better addressed. One of these, investigated here, is the choice of electronic entropy in Born-Oppenheimer MD simulation carried out in the microcanonical ensemble when $K + \Omega$ is a conserved and hence T_{el} is kept fixed along the Hellmann-Feynman trajectory. Since melting is accompanied by a large drop in temperature we

need to quantify the errors introduced due to the choice of electronic temperature/entropy. We, therefore, compare the melting temperature calculated using $T_{\text{el}} \approx T_{\text{h}}$ and $T_{\text{el}} \approx T_{\text{m}}$ since these represent reasonable upper and lower bounds to the "true" melting temperature. For SiO_2 and CaSiO_3 at high pressure and temperature, the difference in the calculated T_{m} with $T_{\text{el}} \approx T_{\text{h}}$ and $T_{\text{el}} \approx T_{\text{m}}$ is about 200-300 K. Although these discrepancies are only a few percent of the melting temperature, they are not negligible for the accurate calculation of melting temperature and are important to take into account for a critical assessment of the Z method implemented together with Born-Oppenheimer MD in the

NVE ensemble with a constant electronic temperature.

ACKNOWLEDGMENTS

We thank Prof. Dario Alfé for the thoughtful discussion. The Centre for Earth Evolution and Dynamics is funded by the Research Council of Norway through its Centre of Excellence program (Grant 223272). We acknowledge financial support from the Research Council of Norway through its Centres of Excellence scheme, project number 332523 (PHAB). Computational resources were provided by the Norwegian infrastructure for high-performance computing (NOTUR, Sigma-2, Grants NN9329K and NN2916K).

-
- [1] A. B. Belonoshko, N. V. Skorodumova, A. Rosengren, and B. Johansson, Melting and critical superheating, *Physical Review B* **73**, 012201 (2006).
- [2] V. Olguín-Arias, S. Davis, and G. Gutierrez, Extended correlations in the critical superheated solid, *The Journal of Chemical Physics* **151**, 10.1063/1.5111527 (2019).
- [3] C. J. Rossouw and S. E. Donnelly, Superheating of small solid-argon bubbles in aluminum, *Phys. Rev. Lett.* **55**, 2960 (1985).
- [4] J. B. Boyce and M. Stutzmann, Orientational Ordering and Melting of Molecular H_2 in an α -Si Matrix: NMR Studies, *Physical Review Letters* **54**, 562 (1985).
- [5] R. W. Cahn, Materials science: Melting and the surface, *Nature* **323**, 668 (1986).
- [6] J. H. Evans and D. J. Mazey, Solid bubble formation in titanium injected with krypton ions, *Journal of Nuclear Materials* **138**, 176 (1986).
- [7] M. Z. Mo, Z. Chen, R. K. Li, M. Dunning, B. B. L. Witte, J. K. Baldwin, L. B. Fletcher, J. B. Kim, A. Ng, R. Redmer, A. H. Reid, P. Shekhar, X. Z. Shen, M. Shen, K. Sokolowski-Tinten, Y. Y. Tsui, Y. Q. Wang, Q. Zheng, X. J. Wang, and S. H. Glenzer, Heterogeneous to homogeneous melting transition visualized with ultrafast electron diffraction, *Science* **360**, 1451 (2018).
- [8] A. R. Finney and P. M. Rodger, Applying the Z method to estimate temperatures of melting in structure II clathrate hydrates, *Physical Chemistry Chemical Physics* **13**, 19979 (2011).
- [9] B. K. Benazzouz, A. Zaoui, and A. B. Belonoshko, Determination of the melting temperature of kaolinite by means of the Z-method, *American Mineralogist* **98**, 1881 (2013).
- [10] F. Saiz, An ab initio study on liquid silicon carbide, *Journal of Physics and Chemistry of Solids* **137**, 109204 (2020).
- [11] S. R. Baty, L. Burakovsky, and D. Errandonea, Ab initio phase diagram of silver, *Journal of Physics: Condensed Matter* **33**, 485901 (2021).
- [12] J. Bouchet, F. Bottin, G. Jomard, and G. Zerah, Melting curve of aluminum up to 300 GPa obtained through ab initio molecular dynamics simulations, *Physical Review B* **80**, 094102 (2009).
- [13] A. B. Belonoshko and A. Rosengren, High-pressure melting curve of platinum from ab initio z method, *Physical Review B* **85**, 174104 (2012).
- [14] H. Y. Geng, R. Hoffmann, and Q. Wu, Lattice stability and high-pressure melting mechanism of dense hydrogen up to 1.5 tpa, *Physical Review B* **92**, 104103 (2015).
- [15] L. Burakovsky, N. Burakovsky, and D. L. Preston, Ab initio melting curve of osmium, *Physical Review B* **92**, 174105 (2015).
- [16] Y. Zhang, Y. Tan, H. Y. Geng, N. P. Salke, Z. Gao, J. Li, T. Sekine, Q. Wang, E. Greenberg, V. B. Prakapenka, and J.-F. Lin, Melting curve of vanadium up to 256 gpa: Consistency between experiments and theory, *Physical Review B* **102**, 214104 (2020).
- [17] D. V. Minakov, M. A. Paramonov, G. S. Demyanov, V. B. Fokin, and P. R. Levashov, Ab initio calculation of hafnium and zirconium melting curves via the lindemann criterion, *Physical Review B* **106**, 214105 (2022).
- [18] J. Braithwaite and L. Stixrude, Melting of CaSiO_3 perovskite at high pressure, *Geophysical Research Letters* **46**, 2037 (2019).
- [19] S. M. Stishov, I. N. Makarenko, V. A. Ivanov, and A. M. Nikolaenko, On the entropy of melting, *Physics Letters A* **45**, 18 (1973).
- [20] S. Davis, S. , Loyola, and P. J., Bayesian statistical modeling of microcanonical melting times at the superheated regime, *Physica A* **515**, 546 (2019).
- [21] D. Alfé, C. Cazorla, and M. J. Gillan, The kinetics of homogeneous melting beyond the limit of superheating, *The Journal of Chemical Physics* **135**, 024102 (2011).
- [22] F. González-Cataldo, S. Davis, and G. Gutierrez, Z method calculations to determine the melting curve of silica at high pressures, *Journal of Physics: Conference Series* **720**, 012032 (2016).
- [23] J.-A. Hernandez, C. E. Mohn, M. G. Guren, M. A. Baron, and R. G. Trønnes, Ab initio atomistic simulations of ca-perovskite melting, *Geophysical Research Letters* **49**, e2021GL097262 (2022).
- [24] C. Di Paola and J. P. Brodholt, Modeling the melting of multicomponent systems: the case of MgSiO_3 perovskite under lower mantle conditions, *Scientific Reports* **6**, 29830 (2016).
- [25] B. Grabowski, L. Ismer, T. Hickel, and J. Neugebauer, Ab initio up to the melting point: Anharmonicity and

- vacancies in aluminum, *Physical Review B* **79**, 134106 (2009).
- [26] A. I. Duff, T. Davey, D. Korbmayer, A. Glensk, B. Grabowski, J. Neugebauer, and M. W. Finnis, Improved method of calculating ab initio high-temperature thermodynamic properties with application to zrc, *Physical Review B* **91**, 214311 (2015).
- [27] S.-T. Lin, M. Blanco, and I. Goddard, William A., The two-phase model for calculating thermodynamic properties of liquids from molecular dynamics: Validation for the phase diagram of lennard-jones fluids, *The Journal of Chemical Physics* **119**, 11792 (2003).
- [28] L.-F. Zhu, B. Grabowski, and J. Neugebauer, Efficient approach to compute melting properties fully from ab initio with application to cu, *Physical Review B* **96**, 224202 (2017).
- [29] A. de Vita, The energetics of defects and impurities in metal and ionic materials from first principles, PhD Thesis, Keele University (1992).
- [30] R. M. Wentzcovitch, J. L. Martins, and P. B. Allen, Energy versus free-energy conservation in first-principles molecular dynamics, *Physical Review B* **45**, 11372 (1992).
- [31] M. Weinert and J. W. Davenport, Fractional occupations and density-functional energies and forces, *Physical Review B* **45**, 13709 (1992).
- [32] A. Corgne, C. Liebske, B. J. Wood, D. C. Rubie, and D. J. Frost, Silicate perovskite-melt partitioning of trace elements and geochemical signature of a deep perovskitic reservoir, *Geochimica et Cosmochimica Acta* **69**, 485 (2005).
- [33] S. Tateno, K. Hirose, S. Sakata, K. Yonemitsu, H. Ozawa, T. Hirata, N. Hirao, and Y. Ohishi, Melting phase relations and element partitioning in morb to lowermost mantle conditions, *Journal of Geophysical Research: Solid Earth* **123**, 5515 (2018).
- [34] P. K. Das, C. E. Mohn, J. P. Brodholt, and R. G. Trønnes, High-pressure silica phase transitions: Implications for deep mantle dynamics and silica crystallization in the protocore, *American Mineralogist* **105**, 1014 (2020).
- [35] F. González-Cataldo, S. Davis, and G. Gutierrez, Melting curve of SiO₂ at multimegabar pressures: implications for gas giants and super-earths, *Scientific Reports* **6**, 26537 (2016).
- [36] K. Hirose, Crystallization of silicon dioxide and compositional evolution of the earth's core, *Nature* **543**, 99 (2017).
- [37] R. G. Trønnes, M. A. Baron, K. R. Eigenmann, M. G. Guren, B. H. Heyn, A. Løken, and C. E. Mohn, Core formation, mantle differentiation and core-mantle interaction within earth and the terrestrial planets, *Tectonophysics* **760**, 165 (2019).
- [38] N. D. Mermin, Thermal properties of the inhomogeneous electron gas, *Physical Review* **137**, A1441 (1965).
- [39] G. Kresse and J. Hafner, Ab initio molecular dynamics for liquid metals, *Physical Review B* **47**, 558 (1993).
- [40] G. Kresse and J. Hafner, Ab initio molecular-dynamics simulation of the liquid-metal-amorphous-semiconductor transition in germanium, *Physical Review B* **49**, 14251 (1994).
- [41] P. E. Blöchl, Projector augmented-wave method, *Physical Review B* **50**, 17953 (1994).
- [42] G. Kresse and D. Joubert, From ultrasoft pseudopotentials to the projector augmented-wave method, *Physical Review B* **59**, 1758 (1999).
- [43] J. P. Perdew, K. Burke, and M. Ernzerhof, Generalized gradient approximation made simple, *Physical Review Letters* **77**, 3865 (1996).
- [44] R. Armiento and A. E. Mattsson, Functional designed to include surface effects in self-consistent density functional theory, *Phys. Rev. B* **72**, 085108 (2005).
- [45] D. Alfè, Melting curve of MgO from first-principles simulations, *Phys. Rev. Lett.* **94**, 235701 (2005).
- [46] A. B. Belonoshko and L. S. Dubrovinsky, Molecular dynamics of stishovite melting, *Geochimica et Cosmochimica Acta* **59**, 1883 (1995).
- [47] Y. Usui and T. Tsuchiya, Ab initio two-phase molecular dynamics on the melting curve of SiO₂, *Journal of Earth Science* **21**, 801 (2010).
- [48] M. Millot, N. Dubrovinskaia, A. Černok, S. Blaha, L. Dubrovinsky, D. G. Braun, P. M. Celliers, G. W. Collins, J. H. Eggert, and R. Jeanloz, Shock compression of stishovite and melting of silica at planetary interior conditions, *Science* **347**, 418 (2015).
- [49] D. Andraut, L. Pison, G. Morard, G. Garbarino, M. Mezouar, M. A. Bouhifd, and T. Kawamoto, Comment on: Melting behavior of SiO₂ up to 120 GPa (andraut et al. 2020), *Physics and Chemistry of Minerals* **49**, 3 (2022).
- [50] D. Andraut, G. Morard, G. Garbarino, M. Mezouar, M. A. Bouhifd, and T. Kawamoto, Melting behavior of SiO₂ up to 120 GPa, *Physics and Chemistry of Minerals* **47**, 10 (2020).
- [51] Q.-J. Hong and A. van de Walle, A user guide for sluschi: Solid and liquid in ultra small coexistence with hovering interfaces, *Calphad* **52**, 88 (2016).
- [52] Y. Shen, S. B. Jester, T. Qi, and E. J. Reed, Nanosecond homogeneous nucleation and crystal growth in shock-compressed SiO₂, *Nature Materials* **15**, 60 (2016).
- [53] S. Wang, G. Zhang, H. Liu, and H. Song, Modified z method to calculate melting curve by molecular dynamics, *The Journal of Chemical Physics* **138**, 134101 (2013).
- [54] A. V. Karavaev, V. V. Dremov, and T. A. Pravishkina, Precise calculation of melting curves by molecular dynamics, *Computational Materials Science* **124**, 335 (2016).
- [55] C. E. Mohn, S. Stølen, and S. Hull, Diffusion within α -CuI studied using ab initio molecular dynamics simulations, *Journal of Physics: Condensed Matter* **21**, 335403 (2009).
- [56] C. E. Mohn, S. Stølen, S. T. Norberg, and S. Hull, Ab initio molecular dynamics simulations of oxide-ion disorder in the δ -Bi₂O₃, *Phys. Rev. B* **80**, 024205 (2009).
- [57] D. Alfè, M. J. Gillan, and G. D. Price, Complementary approaches to the ab initio calculation of melting properties, *The Journal of Chemical Physics* **116**, 6170 (2002).
- [58] A. Wilson and L. Stixrude, Entropy, dynamics, and freezing of CaSiO₃ liquid, *Geochimica et Cosmochimica Acta* **302**, 1 (2021).
- [59] G. Zhang, X. Fan, Q. Zhang, Q. Li, Y. Wu, and M. Li, Partial disordering and homogeneous melting in multi-component systems, *Acta Materialia* **239**, 118281 (2022).
- [60] A. B. Belonoshko, L. Burakovsky, S. P. Chen, B. Johansson, A. S. Mikhaylushkin, D. L. Preston, S. I. Simak, and D. C. Swift, Molybdenum at high pressure and temperature: Melting from another solid phase, *Physical Review*

Letters **100**, 135701 (2008).

- [61] A. D. Rabuck and G. E. Scuseria, Improving self-consistent field convergence by varying occupation numbers, *The Journal of Chemical Physics* **110**, 695 (1999).
- [62] G. Kresse and J. Furthmüller, Efficient iterative schemes for ab initio total-energy calculations using a plane-wave basis set, *Physical Review B* **54**, 11169 (1996).
- [63] G. Kresse and J. Furthmüller, Efficiency of ab-initio total energy calculations for metals and semiconductors using a plane-wave basis set, *Computational Materials Science* **6**, 15 (1996).
- [64] G. Levi, A. V. Ivanov, and H. Jónsson, Variational density functional calculations of excited states via direct optimization, *Journal of Chemical Theory and Computation* **16**, 6968 (2020).
- [65] M. R. Pederson and K. A. Jackson, Pseudoenergies for simulations on metallic systems, *Physical Review B* **43**, 7312 (1991).

Influence of electronic entropy on Hellmann-Feynman forces in *ab initio* molecular dynamics with large temperature changes

Supplementary Information

Ming Geng¹ and Chris E. Mohn^{1,2,*}

¹The Centre for Earth Evolution and Dynamics (CEED) and Centre for Planetary Habitability (PHAB), University of Oslo, N-0315 Oslo, Norway and

²Department of Chemistry and Center for Materials Science and Nanotechnology, University of Oslo, Oslo 0371, Norway

A. Distribution of waiting times and mean errors in the calculated melting temperature

The use of a waiting time analysis via Eq. 3 provides a powerful implementation of the Z method, but many MD runs is still needed for the precise calculation of T_m . In Figs. S1 and S2 we show the convergence of the melting temperature with number of sets where each "set" contains one MD run from each initial temperature. This shows that about 10 simulations of each set (about 30 MD runs in total) gives mean errors of less than 100 K. However many of these runs lasted for more than 200 ps and more MD runs would have been beneficial, in particular close to the melting temperature. Although the stochastic nature of melt nucleation and long tails in the waiting time distribution remains a challenge to the Z method [20, 21], the emergence of machine learning could provide a powerful future approach to improve statistics [39, 40].

The stochastic nature of melting is illustrated as an inset in Fig. S3. Here we show the time evolution of a number of MD runs with the same total energy, E , which is slightly above E_h . As seen, some calculations melted fairly quickly (< 10 ps) whereas others remained stable for more the 200 ps. Although we do not have sufficient statistics to capture the functional form of the distribution of τ , analysis carried out by Davis *et al* [20] showed - using a classical Lennard-Jones potential to model melting of Ar - that the distribution of waiting times appears to deviate markedly from that of an exponential decay.

Although exponential decays describe many dynamical atomistic processes such as hopping events in solids [55, 56], the time taken from random fluctuations that trigger melting to when melting is observed will always take a certain time [20]. This suggests that τ deviates from an exponential decay at short times [20]. In Fig. S3 and S4, we plot the distribution of the waiting times and possible (fitted) distributions for CaSiO_3 and SiO_2 respectively. The plots confirm that the melting time is sensitive to initial temperature and electronic entropy as discussed above. The distributions of τ with T_{el} close to T_m are wide and with standard deviations which are on the size of the average waiting time. For CaSiO_3 runs (with $T_{ini} = 20000$ K and $T_{el} = 6500$ K), for example, the mean

waiting time is ~ 50 ps with standard deviations of similar size when taken from a normal distribution as shown in Fig. S3.

If we assume that the melting temperature can be precisely determined by Eq. 3, a fruitful strategy to minimize the computational cost in a waiting time analysis would be to choose the total energies/initial temperatures such that $\langle \tau \rangle < 10$ ps and $\tau > \tau_{\text{melting}} \approx 1$ ps. The upper bound ensures that we minimize lengthy MD runs, whereas the lower bound, τ_{melting} , ensures that the waiting time is markedly longer than the time it takes from liquid precursors is formed until the entire system has melted which, in our cases where rather small simulations boxes have been used, are typical ~ 1 ps. (see Fig. 1 in the main text). If the waiting time is shorter than the melting time, it is difficult to precisely identify the waiting time in a given run and hence the error bars in $\langle \tau \rangle^{-1/2}$ are large (as seen in Fig. 4 in the main text at short waiting times).

B. Solid-liquid oscillations

Although solid-liquid transitions may be triggered by small changes in electronic entropy, refreezing can also occur spontaneously in NVE runs when the temperature fluctuations are large. That is, when there is an overlap between liquid and solid temperature distributions as discussed in Ref. [21]. Fig. S5 illustrates solid-liquid oscillations for SiO_2 . Here the temperature drops after about 20 ps as the system melts, followed by a 30 ps evolution in the liquid state before the system rapidly recrystallizes. After 10 ps in the solid state, it melts again and remains stable in the melt for more than 20 ps before the run is terminated. Since, however, the temperature fluctuations scale as $1/\sqrt{N}$ (where N is the number of atoms in the simulation box), the overlap between the solid and liquid temperatures decreases with increasing box size and hence the frequency of the solid-liquid alternation decreases. Oscillation on a time scale of nanoseconds or less is therefore usually only seen in MD runs carried out in small simulation boxes (~ 100 atoms).

An interesting implication of such solid-liquid oscillation is that it is possible to estimate the melting temperature by targeting the total energy in which the system spends an equal amount of time in the solid and liquid phases. In this case, the entropy of the two phases

* chrism@kjemi.uio.no

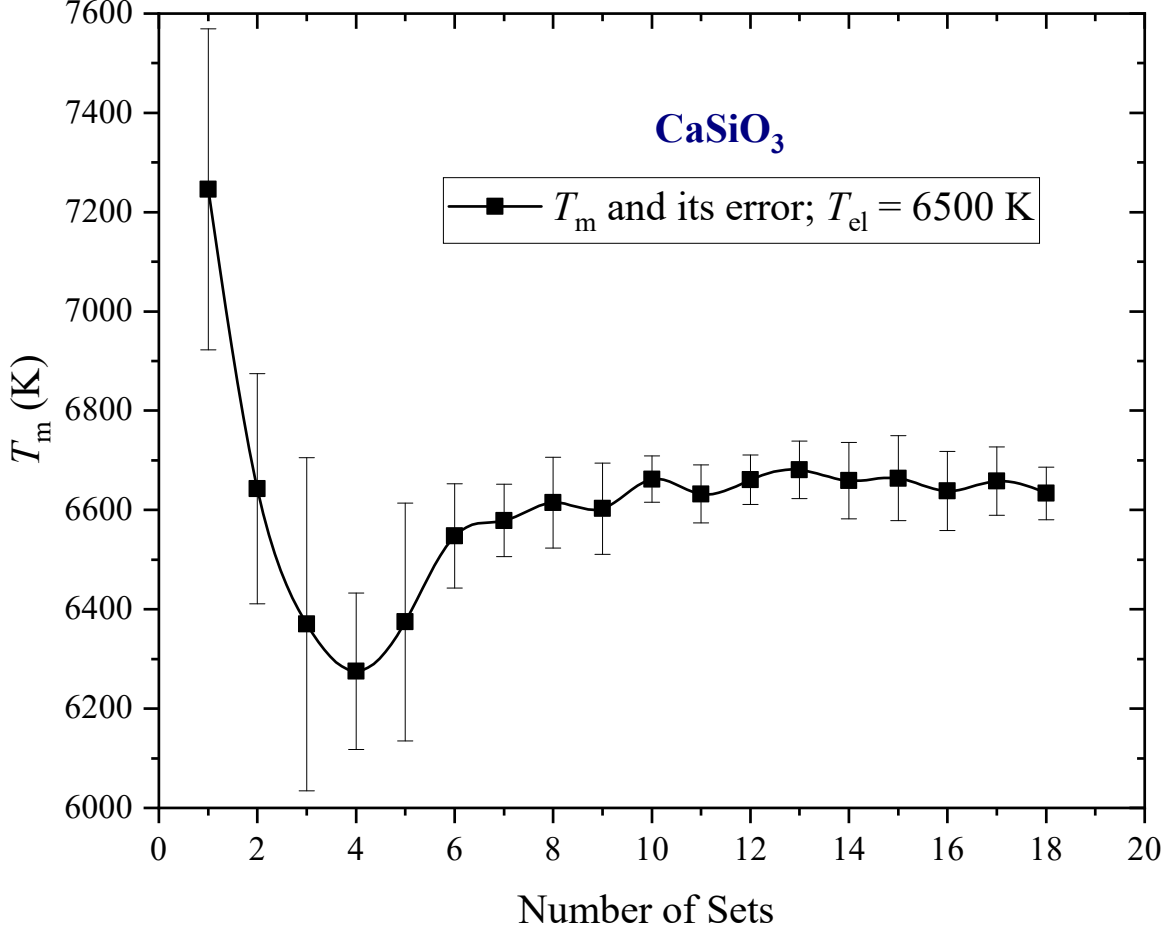


FIG. S1. Convergence of T_m with number of MD runs for CaSiO_3 . Each "set" of MD runs contains three different initial temperatures.

are equal and hence the melting temperature can be extracted directly from the average temperature in the liquid state [21]. However, in our case of SiO_2 melting at ~ 160 GPa, extremely long runs - probably on the size of tens of nanoseconds - would be needed to collect sufficient statistics. In addition, analysis of all trajectories shows that liquid-solid transition is rare in *NVE* MD runs in SiO_2 , and for CaSiO_3 we did not observe any

re-crystallization events even though the size of the simulation box size is modest (135 atoms). The emergence of machine learning with "on the fly" construction of force-fields along the MD trajectory could provide a powerful future implementation of the Z method to improve statistics. This would enable one to explore such oscillations on much longer time-scales than that possible with conventional BOMD simulations.

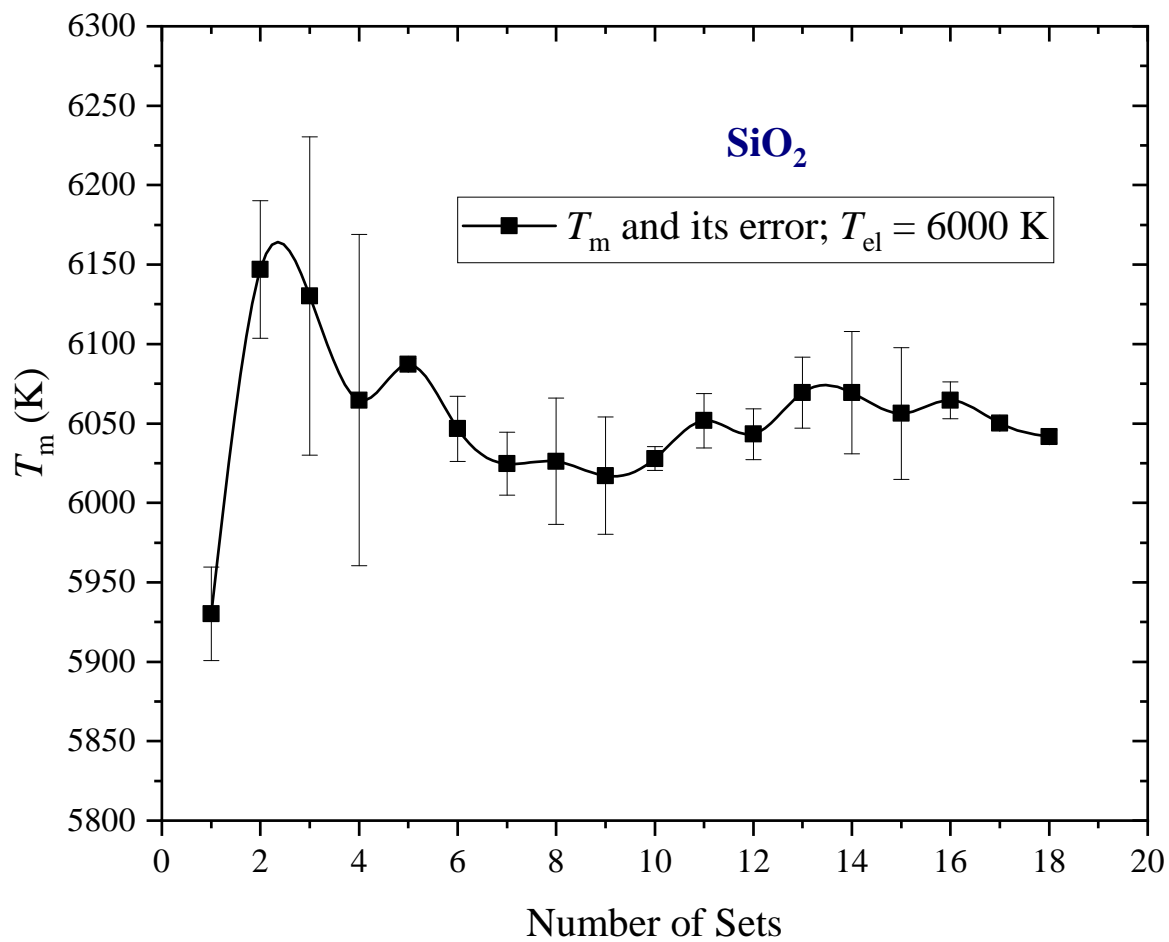


FIG. S2. Convergence of T_m with number of MD runs for SiO₂. Each "set" of MD runs contains three different initial temperatures.

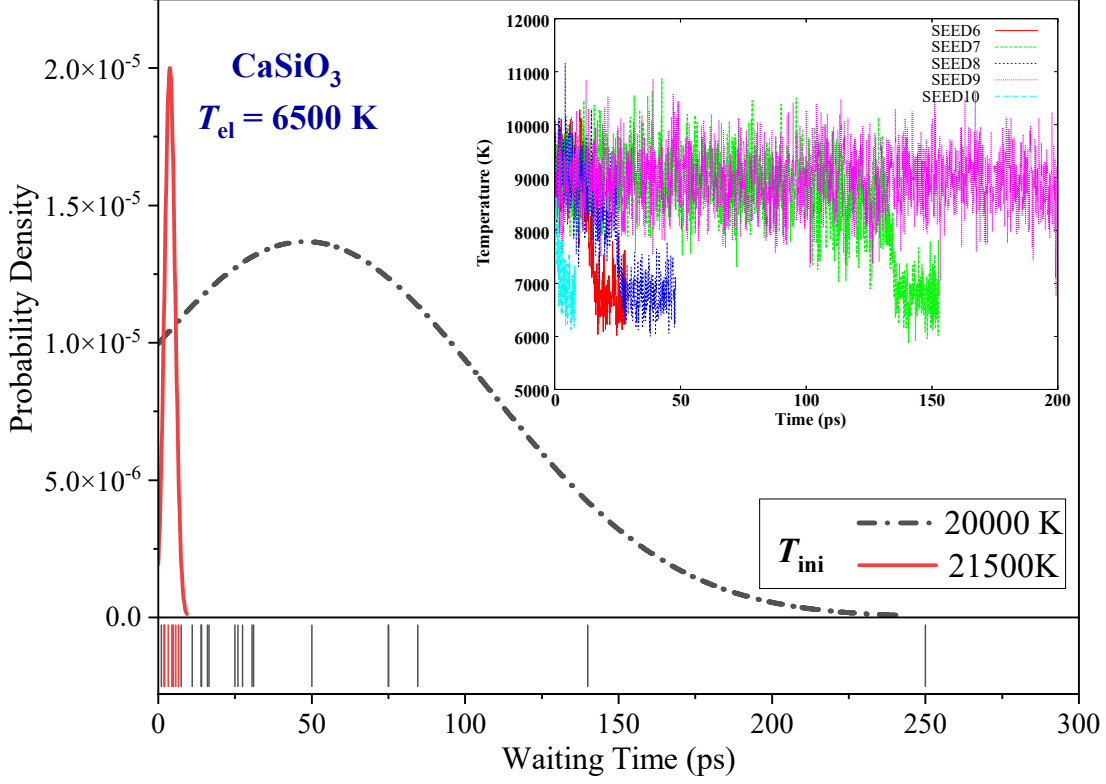


FIG. S3. Distribution of waiting times for melting and examples of *NVE* MD runs of CaSiO_3 with $T_{\text{ini}} = 20000$ K and $T_{\text{el}} = 6500$ K. A normal-distribution is fitted to the distribution probability density. The inset figure shows five different seeds of the temperature evolution in an *NVE* MD runs with $E > E_h$ for CaSiO_3 . In all runs the atoms were located at their equilibrium positions and the velocities were drawn from a Maxwell-Boltzmann distribution.

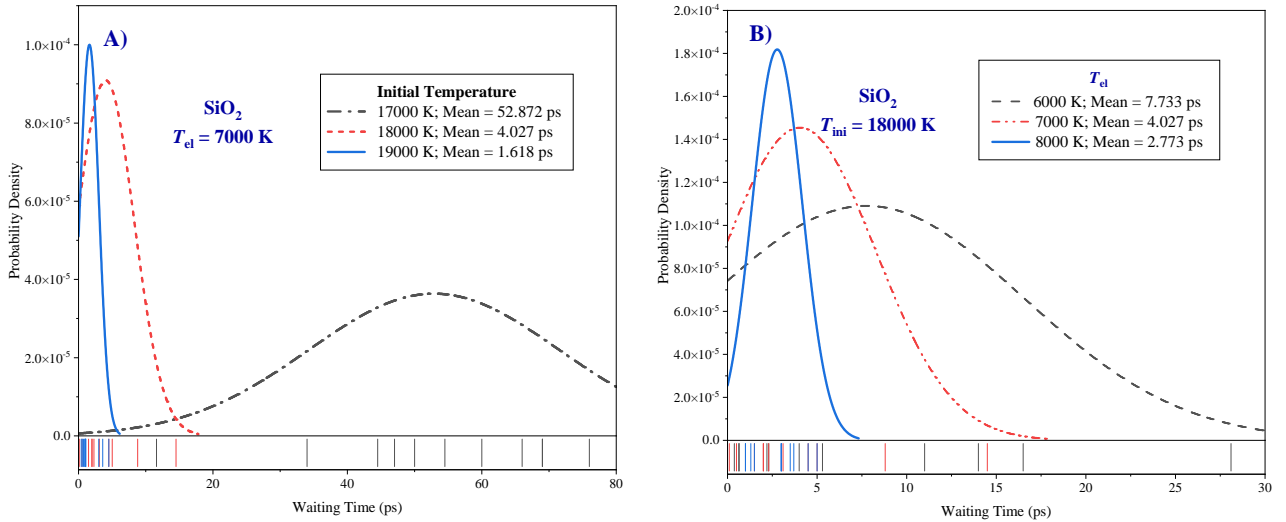


FIG. S4. Distribution of waiting times for melting of SiO_2 . A function is fitted to the distribution probability density. In the left figure we show distributions from runs with the same electronic temperature but different initial temperature and in the right one the initial temperatures are the same but the electronic temperatures are different. In all runs, the atoms were located at their equilibrium positions and the velocities were drawn from a Maxwell-Boltzmann distribution.

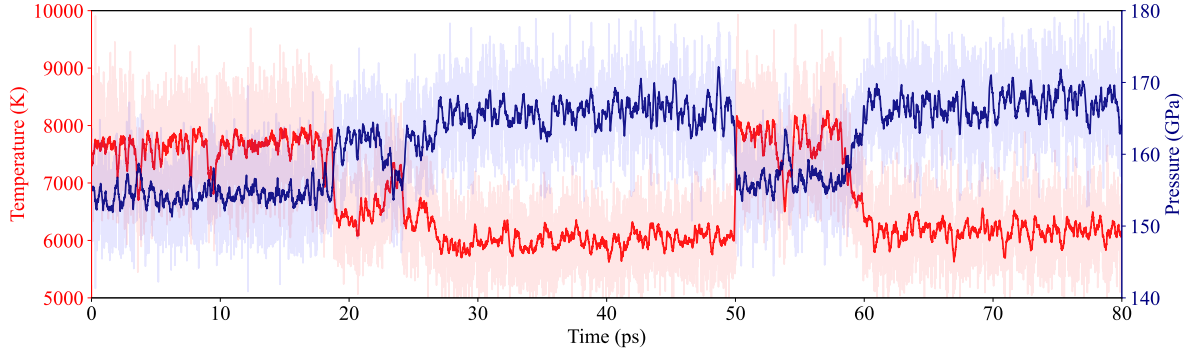


FIG. S5. Temperature and pressure evolution in an SiO_2 MD run where $T_{\text{ini}} = 17000$ K and $T_{\text{el}} = 8000$ K. Transition between liquid and solids take place at 25 ps, 50 ps and 60 ps. Note the overlapping fluctuations in temperature/pressure along solid and liquid states.